Effect of nitrogen or boron impurities on the mechanical and vibrational properties of graphene nanosheets: a molecular dynamics approach

Mahboube Mehrabani[1], *Mohammad Mahdi Khatibi*[2] ✉, *Mohammad Reza Ashory*[2], *Sadegh Sadeghzadeh*[3]

[1]*Mechanical Engineering Department, Semnan University, Semnan, P.O. Box 3513119111, Iran*
[2]*Faculty of Mechanical Engineering, Semnan University, Semnan, P.O. Box 3513119111, Iran*
[3]*Nanotechnology Department, School of New Technologies, Iran University of Science and Technology (IUST), Tehran, P.O. Box 1684613114, Iran*
✉ *E-mail: mmkhatibi@semnan.ac.ir*

Published in Micro & Nano Letters; Received on 18th January 2020; Revised on 25th April 2020; Accepted on 6th May 2020

Investigation of mechanical and vibrational properties of nano-structures using the analytical methods would be time-consuming. Therefore, using a semi-empirical method would reduce the time needed to investigate materials characterisation. One of the semi-empirical approaches is molecular dynamics. In this Letter, the large-scale atomic/molecular massively parallel simulator software is used to simulate the mechanical and vibrational behaviour of a nitrogen- and boron-doped 24.04 × 51.13 Å graphene nano-sheet. The natural frequencies, Young's modulus, and ultimate tensile strength (UTS) are studied. By adding impurity to the nanosheet and increasing its density, Young's modulus, UTS, and natural frequencies were decreased. The decrease in tensile properties was more significant in the case of boron impurity. When the boron (nitrogen) impurity increased to about 20%, Young's modulus and the first natural frequency were decreased 7.1% (9%) and 16.8% (73%), respectively. This illustrates that Young's modulus and natural frequencies are directly related. Therefore, for the same dimensions and boundary conditions, it is obvious that the increase in impurity content has reduced the natural frequencies of the nanostructure.

1. Introduction: Graphene is one of the main allotropes of carbon in the single-layer state which has shown fascinating applications in bioelectronics [1]. The recent applications of graphene have been in different fields such as sensors, energy storage devices, polymer composites, and nano-composites [2]. Many efforts have been conducted to improve the electrical and mechanical properties of graphene sheets. Chemical doping with other atoms is an effective method to intrinsically modify the properties of base materials [3]. Nitrogen and boron doping play a critical role in regulating the electronic and mechanical properties of carbon-based materials. They are excellent elements because of their close atomic size and strong valence bonds with carbon atoms [4]. Nitrogen- and boron-doped graphene is usually promising for applications in electrochemical energy devices such as lithium-ion batteries [5] and biosensors [6]. Carbon nitride- and boron-based nanostructures have attracted special attention (from theory and experimental aspects) due to their remarkable electromechanical properties [7]. Many kinds of research studies have been conducted to clarify the mechanical properties of nano-structures using different analytical methods such as strain gradient theory [8], fully gradient elasticity [9, 10], Eringen differential models [11, 12], energy equivalent model [13], non-local or surface elasticity [14], and other theoretical and even experimental methods [15–17]. Furthermore, non-local theories are also one of the common methods for modelling discontinuous nano-structures, which make continuum theories suitable for the analysis of such nano-structures. Some of these non-local theories are investigated in research studies [18–20].

As mentioned, in some of the research studies, the analytical methods have been used while in some other molecular dynamics (MD) simulations have been utilised to derive the mechanical behaviour of N- and B-doped graphene. Some of these studies were summarised as follows.

De Sousa *et al.* [7] investigated the mechanical properties and fracture mechanisms of three different structures of nitrogen-doped graphene families at three different temperatures including 10, 300, and 600 K. They observed that Young's modulus for the carbon nitride membranes is smaller than the intrinsic graphene.

Ghorbanfekr *et al.* [21] studied the mechanical properties of N-doped graphene using a reactive force field (ReaxFF) potentials. They illustrated that the formation energy and the N/C ratio are directly related. While Young's modulus, tensile strength, and intrinsic strain decreased with the increase in the number of nitrogen atoms.

Han *et al.* [22] investigated the mechanical properties of graphene sheets doped with silicon, nitrogen, or boron atoms. They studied Young's modulus, ultimate stress (strain), and energy adsorption for the graphene sheets with the doping concentration ranging from 0 to 5%. It is noted that stress (s) is a physical quantity that expresses the internal forces that neighbouring particles of a material exert on each other in the unit area, while strain (e) is the measure of the deformation of the material in the unit length. Furthermore, the ultimate tensile strength (UTS) is the maximum stress that the material will endure before fracture. They concluded that incorporating the dopants into the graphene sheet has led to an almost linear decrease in Young's modulus and monotonic reductions in ultimate strength, ultimate strain, and energy adsorption. Such doping effects were found to be most significant for silicon, less pronounced for boron, and negligible for nitrogen.

Mortazavi *et al.* [23] investigated the effects of doped nitrogen atoms on Young's modulus and tensile strength of graphene, using MD simulations. They concluded that Young's modulus of N-doped graphene was almost independent of nitrogen atoms concentration (up to 6%). On the other hand, substituted nitrogen atoms decreased tensile strength.

Okamoto and Ito [24] studied the effects of nitrogen content and different distributions of nitrogen atoms in graphene on its properties using different types of potential functions. They observed that the strength and Young's modulus did not change much for a nitrogen content of up to 4% unless two nitrogen atoms present in graphene adjoin each other.

Chan and Hill [25] investigated the interaction of various atoms/ions with a graphene sheet and two parallel graphene sheets using the Lennard–Jones potential.

Mortazavi *et al.* [26] studied the effects of substitution of boron atoms in graphene nanosheet on the thermal conductivity and

mechanical properties of single-layer graphene using the non-equilibrium MD simulations. They found that increasing boron concentration change the failure behaviour of graphene from ductile to brittle, and reduced elastic modulus and tensile strength of graphene.

As consequent, MD is one of the most precise simulation methods in physics that is used to simulate complex multi-particle systems. In this method, phase paths of systems involving thousands of interacting particles are obtained by solving Hamiltonian equations [27] under appropriate boundary conditions. By analysing the particle path in the phase space and applying statistical mechanics, information of various properties of the system including energy, structural, dynamic, mechanical properties etc. will be obtained. In MD simulation, the stepwise configuration of the system is obtained by integrating Newton's laws of motion. The result is a path that shows how the positions and velocities of the system particles change over time. While size-dependent continuum theories (such as strain gradient, non-local elasticity, or surface elasticity) are appropriate for simulating continuous systems, and for discontinuous systems, non-local coefficients are applied to that of equations, as is studied in the literature [28–32]. Non-local coefficient extraction is beyond the scope of this Letter.

Based on the literature review, a conclusion could be presented as follows:

- The mechanical properties (such as Young's modulus, UTS etc.) of graphene up to 6% of nitrogen or boron impurities have been investigated.
- The MD approach is used in the literature, generally.
- In the literature review, the investigation of the vibrational behaviour of graphene-based nanostructures in the MD approach is still rare.

Therefore, the novelty of present research could be described as follows:

- The effect of up to 20% of nitrogen or boron impurities in graphene on mechanical and vibrational properties is studied.
- To derive natural frequencies of nano-structures, the frequency-domain decomposition (FDD) method is used.

Therefore, in this research, mechanical properties and vibrational behaviour of N- and B-doped graphene for various percentages of impurities (up to 20%) are investigated. To obtain the mechanical and vibrational properties of nitrogen-carbon (NC) and boron-carbon (BC) lattice, the MD approach is utilised.

2. Theoretical details

2.1. Molecular dynamics: Experimental investigation of the mechanical and dynamic behaviour of structures in very small scales is very difficult. Therefore, different methods have been used to study mechanical, thermal, and especially vibrational behaviour of structures at very small scales. One of the commonly used procedures is the MD method. MD is a simulation method for studying the movements of atoms in a system of interacting particles, where forces between the particles and their potential energies are often calculated using interatomic potentials or molecular mechanics force fields. In this method, the interaction between particles and the force applied to each atom are calculated using numerically solving Newton's second law of motion equations for a system of interacting particles, as follows:

$$F_i = m_i + a_i \tag{1}$$

where F_i, m_i, and a_i are the force, the mass and the acceleration of the ith particles, respectively. The forces usually derive from potential functions, $U(\boldsymbol{r}_1, \boldsymbol{r}_2, \ldots, \boldsymbol{r}_N)$ using gradient operator (∇), as below [24]

$$\boldsymbol{F}_i(\boldsymbol{r}_1, \boldsymbol{r}_2, \ldots, \boldsymbol{r}_N) = -\nabla_{\boldsymbol{r}_i} U(\boldsymbol{r}_1, \boldsymbol{r}_2, \ldots, \boldsymbol{r}_N) \tag{2}$$

The total conservative energy of a system is represented as follow:

$$E = K + U \tag{3}$$

where 'E', 'K', and 'U' are total energy, total kinetic energy, and total potential energy of atoms' system, respectively. The potential energy in the absence of external forces represents the summation of mutual interactions, as follows [33]:

$$U = \sum_{i=1}^{N} \sum_{j>i}^{N} u\left(\boldsymbol{r}_{ij}\right) \tag{4}$$

where $\boldsymbol{r}_{ij} = \boldsymbol{r}_i - \boldsymbol{r}_j$ is the vector of position, and $u\left(\boldsymbol{r}_{ij}\right)$ is the potential energy of connection between the ith and jth atom. Therefore, the force applied to each atom is represented as follows:

$$\boldsymbol{F}_i = -\sum_{j \neq i}^{N} \frac{\mathrm{d}u\left(\boldsymbol{r}_{ij}\right)}{\mathrm{d}\boldsymbol{r}_{ij}} \tag{5}$$

In this research, a three-dimensional Tersoff potential has been used to determine the interactions between nitrogen or boron and carbon particles in nitrogen-doped and boron-doped graphene structures. This potential function is defined in the literature [26]. The Tersoff potential coefficients are extracted from Kinaci *et al.* [34].

2.2. Vibrational behaviour: In this study, a system of particles was used to simulate the behaviour of carbon structures by doping with boron or nitrogen atoms. The equation of motion for systems consisting of nitrogen particles connected by linear springs to express the scalar displacement of the ith atom is represented as follow [35]:

$$M_i \ddot{u}_i(t) + \sum_j \varphi_{ij} u_j(t) = F_i \tag{6}$$

where M_i is the mass of particle, which is in the position i and φ_{ij} is the stiffness of the spring between particles i and j. At the beginning of the time, the displacement of all particles was zero and an impact force was applied to the graphene nano-sheet in the z-direction. It is noticeable that the x and y axes lie in the sheet, and the z-direction is perpendicular to the sheet. The equation of vibration in the z-direction could be expressed as follows [36]:

$$\rho \frac{\partial^2 z}{\partial t^2} + \frac{D}{h} \nabla^2 z = 0 \tag{7}$$

where ∇^2 is the two-dimensional Laplacian, ρ is the mass density, and h is the thickness of the sheet. Besides, D is the flexural strength, which is defined as follows [36]:

$$D = \frac{Eh^3}{12\left(1 - \nu^2\right)} \tag{8}$$

where E is the modulus of elasticity and ν is Poisson's ratio. In this study, a simply supported boundary condition was selected for a rectangle nano-sheet. The solution of (7) considering simply supported boundary conditions can be found in the literature [37]

doi: 10.1049/mnl.2020.0044

as follows [36]:

$$z_n(t,x,y) = z_0 \sin(k_1 x)\sin(k_2 y)\cos(\omega_n t) \tag{9}$$

$$\omega_n = k_n^2 \sqrt{\frac{Eh^2}{12\rho(1-\nu^2)}} \tag{10}$$

where $k_1 = n_1\pi/a$ and $k_2 = n_2\pi/b$, z_0 is a constant number that represents the amplitude of vibrations and k_n is the amplitude of frequency in the nth mode shape.

2.3. FDD technique: Vibration analysis methods include two categories: parametric and non-parametric. Non-parametric methods extract the dynamic characteristics of the structure by performing mathematical operations on experimental data in the frequency domain [38]. In parametric methods, a parametric model of experimental data for the system is approximated in the time domain and the dynamics model of the system is extracted [39]. One of the non-parametric methods is frequency decomposition. In this method, first, the power spectral density (PSD) matrix of the response is calculated and then, the singular value decomposition method is applied to the PSD matrix. As a result, the values of natural frequencies, damping coefficients, and mode shapes are obtained [40, 41].

The FDD is based on the relationship between the input and output of a system, as follows:

$$\boldsymbol{G}_{yy}(\mathrm{j}\omega) = \bar{\boldsymbol{H}}(\mathrm{j}\omega)\cdot\boldsymbol{G}_{xx}(\mathrm{j}\omega)\cdot\boldsymbol{H}^t(\mathrm{j}\omega) \tag{11}$$

where $\boldsymbol{G}_{xx}$ is the input PSD, $\boldsymbol{G}_{yy}$ is the output PSD, $\boldsymbol{H}$ is the frequency response function (FRF), $\bar{\boldsymbol{H}}$ is the conjugate of $\boldsymbol{H}$, and j is the imaginary unit. The FRF could be expressed as follows [42]:

$$\boldsymbol{H}(\mathrm{j}\omega) = \sum_{k=1}^{n}\frac{Q_k}{\mathrm{j}\omega-\lambda_k} + \frac{\bar{Q}_k}{\mathrm{j}\omega-\bar{\lambda}_k} \tag{12}$$

where Q_k is a residual term, $\bar{Q}_k$ is the conjugate of Q_k, λ_k is the kth natural frequency, n is the number of available modes. By inserting (12) into (11), and after using mode shapes orthogonality, the PSD could be represented as follows:

$$\boldsymbol{G}_{yy}(\mathrm{j}\omega) = \sum_{k=1}^{n}\frac{d_k\boldsymbol{\phi}_k\boldsymbol{\phi}_k^t}{\mathrm{j}\omega-\lambda_k} + \frac{\bar{d}_k\bar{\boldsymbol{\phi}}_k\bar{\boldsymbol{\phi}}_k^t}{\mathrm{j}\omega-\bar{\lambda}_k} \tag{13}$$

where d_k represents a scalar and $\boldsymbol{f}_k$ is the kth mode shape vector. According to (13), at each frequency, a limited number of modes have contributed in the construction of the system response. Near the natural frequencies of the system, only one mode has a significant role in the construction of the system response; besides, system response at this frequency (near the natural frequencies) would be similar to the mode shape at this frequency.

3. Calculation procedure: In this study, simulations are done with the MD approach using large-scale atomic/molecular massively parallel simulator (LAMMPS) software. LAMMPS is a classical MD code with a focus on materials modelling [43]. LAMMPS is written in C++ and it is an open-source code [44]. It can be used to model atoms or, more generically, as a parallel particle simulator at the atomic or continuum scale [43]. To model a rectangular sheet in MD virtual laboratory, particles such as carbon, nitrogen, and boron are arranged in a hexagonal lattice form. The lattice has 480 atoms and its dimension is 24.04×51.13 Å. A simulation box with a size greater than C–N and C–B structures in all directions has been created. One row of the boundary atoms of the system is fixed owing to applying a simply support boundary condition for a structure, in the case of the vibrational analysis. It is noticeable that fixing more than one row does not satisfy the clamped condition [33, 45, 46]. The different impurity percentage of 0, 1, 5, 10, and 20% are selected to investigate the effects of N- and B-doping percentage on mechanical and vibrational behaviour of graphene nano-sheet as shown in Fig. 1. In this figure, red points represent carbon particles and blue points indicate impurity particles. Impurity or dopant particles are substituted randomly in the graphene nano-sheet by carbon atoms. As shown in this figure, the outer row of particles that are connected with a continuous black line is fixed to satisfy the simply supported boundary condition.

It is worth mentioning that to consider the effects of impurity random distribution, the simulation is executed six times in the different forms of impurity particles. Afterwards, the mean value and standard deviation (SD) of results are reported. The SD is represented as follows:

$$\mathrm{SD} = \sqrt{\frac{1}{N-1}\sum_{i=1}^{N}(x_i-\bar{x})^2} \tag{14}$$

where N is the number of data, x_i is the data, and $\bar{x}$ is the mean value of data.

In the simulation, the step-time is selected at 0.0001 ps. To have a system trajectory consistent, the NVE ensemble is used for 1 ps. NVE ensemble represents that the number of atoms (N), the volume of the system (V), and the total energy of the system (E) is fixed during the simulation. Besides, to apply the initial temperature (T) of system, Nose–Hoover thermostat is employed by using the NVT ensemble, for 10,000 step-times. Afterwards, the NVE ensemble is fixed until the end of the simulation process, and a force is applied to the nano-sheet for 0.5 ps to excite the structure for vibrational simulation. Finally, the displacement of particles is measured by sensors. The number of used sensors, the frequency of excitation force, the excitation region and its duration, and data sampling time are important parameters that should be considered to achieve appropriate results [33]. In this simulation, to extract an accurate result, 120 sensors are applied randomly. After measuring the displacement of the particle, the time response of the system to the excitation force is obtained. Also, the frequency response of the system is calculated. Finally, the vibrational properties of the system (such as natural frequencies and mode shapes) are obtained using the FDD technique.

It is noticeable that the simulation of the tensile test in the MD approach has been executed in fixed pressure (P) and temperature (T). Therefore, the NPT ensemble (a Nose–Hoover thermostat and barostat) is used during the tension simulation. The strain rate of nano-sheets during the tensile test simulation is selected as 0.001 s^{-1}, and it is equal to step-time. It is necessary to mention

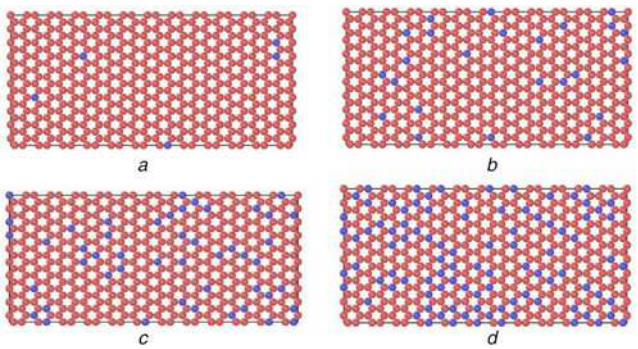

Fig. 1 *Different impurity concentration in graphene nanostructure*
a 1% doped graphene
b 5% doped graphene
c 10% doped graphene
d 20% doped graphene

Table 1 Mechanical properties of pure graphene compared to N- and B-doped graphene

Type of impurity atom	Impurity content	Mechanical properties				Mass, g	Reference
		Young's Modulus, GPa	SD	UTS, GPa	SD		
—	0	1054.10	0	135.56	0	—	[41]
		1086.24	0	134.16	0	5765.28	present work
N	1	1072.66	1.89	129.85	2.86	5775.11	present work
	5	1062.33	3.30	123.58	1.47	5813.04	
	10	1023.75	1.09	117.10	2.55	5861.07	
	20	1009.33	3.49	113.18	2.14	5956.86	
B	1	1061.33	2.53	127.91	2.22	5759.28	present work
	5	1032.00	1.94	116.03	3.05	5736.48	
	10	1001.66	2.34	96.78	2.85	5707.68	
	20	903.32	3.12	75.96	3.95	5650.08	

that the structure is stretched together with the simulation box in the armchair direction.

4. Results and discussions

4.1. Mechanical properties: As the first result, the mechanical properties of graphene nanostructure with different impurity concentrations is simulated using LAMMPS software, and Young's modulus, UTS, and mass of nano-structures are numerically reported in Table 1. It is noticeable that the atomic mass of C, B, and N are 12.0107, 10.8110, and 14.0067 g/mol, respectively [33]. Besides, stress–strain curves of graphene and N- and B-doped graphene in different impurity content is depicted in Fig. 2. Additionally, to better comparison, a bar graph of fracture strain, Young's modulus, and UTS of graphene with impurities have been shown in Figs. 3–5, respectively.

According to Table 1, the MD simulation method, which is utilised in this research, is validated by other research studies [47]. Fig. 2 shows that the fracture strain of graphene is decreased by adding the dopant particle and increasing its concentration. It means that more brittle fracture is observed by increasing impurity percentage as mentioned in the literature [22]. The amount of fracture strain is graphically shown in Fig. 3.

Moreover, by adding the impurities and increasing their percentage, Young's modulus and UTS of graphene are decreased, based on Figs. 4 and 5, respectively. This phenomenon is also reported by Han *et al.* [22]. As is observed in Figs. 4 and 5, adding boron particles is more effective than nitrogen atoms on Young's modulus and UTS of the graphene matrix. It is noticeable that bonding energies of C–C, C–B, and C–N are 607, 448, and

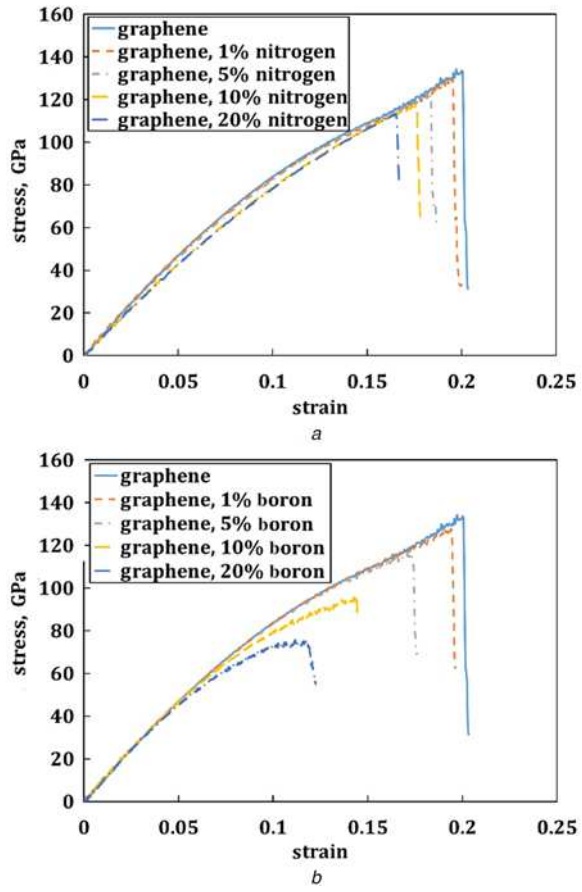

Fig. 2 *Stress–strain curves*
a Nitrogen-doped graphene
b Boron-doped graphene

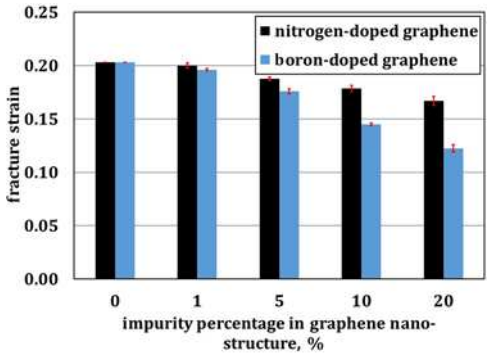

Fig. 3 *Fracture strain of N- and B-doped graphene*

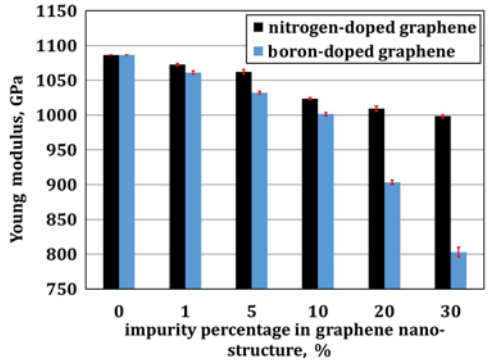

Fig. 4 *Young's modulus of N- and B-doped graphene*

doi: 10.1049/mnl.2020.0044

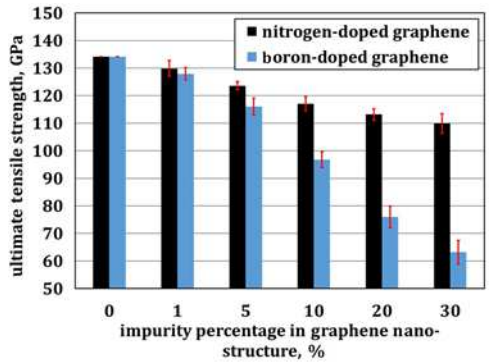

Fig. 5 *UTS of N- and B-doped graphene*

770 kcal/mol, respectively [48]. Based on bonding energies, reduction in UTS and Young's modulus of B-doped graphene is more than N-doped graphene in the same impurity content. Besides, Young's modulus of nitrogen-doped graphene has been reported almost independent of nitrogen atoms concentration (up to 6%), based on the literature [23], because of the difference in nano-structure mass. Therefore, the effect of nitrogen impurity on Young's modulus and UTS is less than boron, in each dopant concentration (up to 20%).

It is noted that the substitution of other particles with carbon particles as impurities in graphene nano-sheet can affect its failure mechanism. As is shown in Fig. 6, the failure has initiated

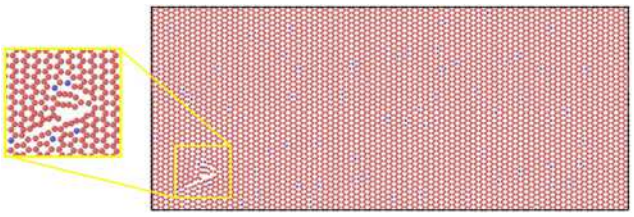

Fig. 6 *Initiation of failure in the graphene nano-sheet with impurities under uniaxial tensile loading*

Table 2 Detail of single-layer graphene sheet [33]

Young's modulus (E), TPa	Poisson ratio, n	Mass density (ρ), kg/m^3	Thickness (h), nm
1.06	0.16	2250	0.34

near impurities. It means that the impurities can cause stress concentration in the nano-structure, because of the difference in size and bond energy. This phenomenon is also observed in the literature [26].

4.2. Vibrational properties: The natural frequencies of rectangular pure graphene (without impurity) are calculated analytically as follows [49]:

$$\omega^2(m,n)=\sqrt{\frac{D\left(\alpha^2+\beta^2\right)^2}{M\lambda}} \tag{15}$$

where m and n are the number of modes in y- and x-directions, respectively. D is defined in (8) and α, b, M, and λ are defined as follows [49]:

$$\alpha=\frac{n\pi}{a} \tag{16}$$

$$\beta=\frac{m\pi}{b} \tag{17}$$

$$\lambda=1+\mu\left(\alpha^2+\beta^2\right) \tag{18}$$

$$M=m_0+m_2\left(\alpha^2+\beta^2\right) \tag{19}$$

where m_0, m_2, and μ represent the mass per unit area, mass moment of inertia, and non-local parameter, respectively. The mechanical properties and thickness (h) of the graphene nano-sheet are reported in Table 2.

The dimensions of the rectangular nano-sheet are 24.04×51.13 Å and its boundary condition is simply supported. The vibrational behaviour of the graphene nano-sheet is investigated, and as a result, the natural frequencies of this nano-sheet are reported in Table 3. It is noted that in this table, the first four natural frequencies of pure graphene are compared to (15) to validate the results of the simulation process. Besides, the natural frequencies of N- and B-doped graphene are reported in Tables 3 and 4.

As is observed in Tables 3 and 4 for a single-layer pure graphene nano-sheet, the result of MD simulation is in good agreement with (15), considering the non-local effect. Therefore, the simulation method has accuracy and is validated. It is noted that the natural frequencies extracted from the non-local model are more accurate compared with the analytical model. The natural frequency of nano-structures is affected by the stiffness and nano-structure mass. The natural frequency is directly related to stiffness and is inversely related to nano-structure mass [50]. It is worthy to mention that stiffness and Young's modulus are directly related [51]. As is shown in Fig. 4, Young's modulus of nano-structure

Table 3 First and second natural frequencies of pure graphene compared to that of N- and B-doped graphene

Type of impurity atom	Impurity content	Natural frequencies, GHz				μ	Reference
		$\omega(1,1)$	SD	$\omega(2,1)$	SD		
—	0	468.2	0	581.3	0	0	[36]
		405.6	0	500.6	0	1	
—	0	405.3	0	498.0	0	1	(17)
N	1	374.3	2.75	485.6	4.35	1	present work
	5	371.7	1.91	472.3	3.91	1	
	10	369.5	3.86	462.7	2.87	1	
	20	368.9	3.73	547.1	1.92	1	
B	1	356.4	1.83	443.6	1.81	1	present work
	5	320.3	1.91	394.8	0.53	1	
	10	246.6	4.68	309.1	3.49	1	
	20	109.5	7.55	160.5	4.10	1	

Table 4 Third and fourth natural frequencies of pure graphene compared to that of N- and B-doped graphene

Type of impurity atom	Impurity content	Natural frequencies, GHz				μ	Reference
		$\omega(3,1)$	SD	$\omega(1,2)$	SD		
—	0	708.5	0	978.6	0	0	[36]
		639.1	0	889.9	0	1	
—	0	637.2	0	886.2	0	1	(15)
N	1	590.4	1.35	726.3	4.13	1	present work
	5	588.7	0.94	728.4	2.80	1	
	10	588.1	1.47	730.4	1.06	1	
	20	587.6	1.45	725.9	5.56	1	
B	1	569.5	2.25	712.1	2.19	1	present work
	5	510.1	3.05	627.6	4.31	1	
	10	405.6	5.48	493.4	6.14	1	
	20	231.3	7.69	330.2	4.37	1	

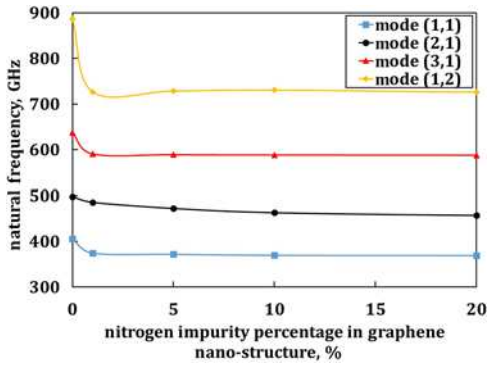

Fig. 7 *Natural frequencies of N-doped graphene nano-sheets with various impurity concentrations subjected to simply supported boundary conditions*

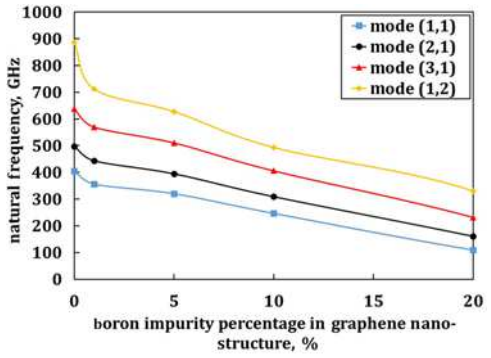

Fig. 8 *Natural frequencies of B-doped graphene nano-sheets with various impurity concentrations subjected to simply supported boundary conditions*

is increased by adding impurity and increasing its percentage. Based on this fact and as mentioned in Table 1, the reduction in natural frequency of N- and B-doped graphene by increasing impurity concentration is reasonable.

As is observed in Fig. 7, the natural frequencies of N-doped graphene is less than the natural frequencies of pure graphene because of its higher mass and lower Young's modulus. Also, as is shown in Fig. 8, the natural frequencies of B-doped graphene is less than the natural frequencies of pure graphene because of its lower Young's modulus. It is noticeable that the mass of B-doped graphene is less than pure graphene, however, the effect of Young's modulus on natural frequency is dominated because of lower C–B bonding energy compared C–C bonding energy. Based on the bonding energy effect, the reduction in natural frequency in N-doped graphene is negligible because of higher C–N bonding energy compared to C–C bonding energy.

5. Conclusion: In this Letter, the effect of nitrogen and boron atoms as an impurity in graphene nano-structure on mechanical and vibrational properties of that nanostructure is investigated using the MD approach in LAMMPS software. This software makes a user-friendly and easy to use interface for applying different potential functions (such as Tersoff, ReaxFF, adaptive intermolecular reactive empirical bond order (AIREBO) etc.) to nano-structures simulation. In this approach, the interaction forces are calculated using an appropriate potential function. Obtained results could be listed as follows:

- Adding nitrogen or boron impurity (up to 20%) to the graphene matrix and increasing its percentage, led to a reduction in fracture strain.

- Young's modulus, UTS, and natural frequencies of graphene are decreased by adding nitrogen or boron impurity and increasing its percentage.

- Adding boron atoms in the graphene matrix is more effective than nitrogen atoms on reduction in Young's modulus, UTS, and natural frequencies.

- The graphene with nitrogen impurity is more suitable than graphene with boron impurity for nano-sensor fabrication, based on natural frequency.

- High natural frequency is an important feature of vibrational sensors. As a result, graphene with nitrogen impurity is more suitable for making nano-sensors than graphene with boron impurities, in the absence of pure graphene.

6 References

[1] Wang Y., Shao Y., Matson D.W., *ET AL.*: 'Nitrogen-doped graphene and its application in electrochemical biosensing', *ACS Nano*, 2010, **4**, (4), pp. 1790–1798

[2] Singh V., Joung D., Zhai L., *ET AL.*: 'Graphene based materials: past, present and future', *Prog. Mater. Sci.*, 2011, **56**, (8), pp. 1178–1271

[3] Sumpter B.G., Meunier V., Herrera J.M.R., *ET AL.*: 'Nitrogen-mediated carbon nanotube growth: diameter reduction, metallicity, bundle dispersability, and bamboo-like structure formation', *ACS Nano*, 2007, **1**, (4), pp. 369–375

[4] Lee S.U., Belosludov R.V., Mizuseki H., *ET AL.*: 'Designing nanogadgetry for nanoelectronic devices with nitrogen-doped capped carbon nanotubes', *Small*, 2009, **5**, (15), pp. 1769–1775

doi: 10.1049/mnl.2020.0044

[5] Wang X., Zeng Z., Ahn H., *ET AL.*: 'First-principles study on the enhancement of lithium storage capacity in boron doped graphene', *Appl. Phys. Lett.*, 2009, **95**, (18), p. 183103
[6] Shao Y., Zhang Sh., Engelhard M.H., *ET AL.*: 'Nitrogen-doped graphene and its electrochemical applications', *J. Mater. Chem.*, 2010, **20**, (35), pp. 7491–7496
[7] de Sousa J., Botari T., Perim E., *ET AL.*: 'Mechanical and structural properties of graphene-like carbon nitride sheets', *RSC Adv.*, 2016, **6**, (80), pp. 76915–76921
[8] Sedighi H.M., Koochi A., Daneshmand F., *ET AL.*: 'Non-linear dynamic instability of a double-sided nano-bridge considering centrifugal force and rarefied gas flow', *Int. J. Non-Linear Mech.*, 2015, **77**, pp. 96–106
[9] Barretta R., Luciano R., de Sciarra F.M.: 'A fully gradient model for Euler–Bernoulli nanobeams', *Math. Probl. Eng.*, 2015, **2015**, Article ID 495095, pp. 1–8
[10] Canadija M., Barretta R., De Sciarra F.M.: 'A gradient elasticity model of Bernoulli–Euler nanobeams in non-isothermal environments', *Eur. J. Mech. A, Solids*, 2016, **55**, pp. 243–255
[11] Demir Ç., Civalek Ö.: 'On the analysis of microbeams', *Int. J. Eng. Sci.*, 2017, **121**, pp. 14–33
[12] Barretta R., Canadija M., de Sciarra F.M.: 'A higher-order Eringen model for Bernoulli–Euler nanobeams', *Arch. Appl. Mech.*, 2016, **86**, (3), pp. 483–495
[13] Eltaher M.A., Agwa M., Kabeel A.: 'Vibration analysis of material size-dependent CNTs using energy equivalent model', *J. Appl. Comput. Mech.*, 2018, **4**, (2), pp. 75–86
[14] Barretta R., de Sciarra F.M.: 'Variational nonlocal gradient elasticity for nano-beams', *Int. J. Eng. Sci.*, 2019, **143**, pp. 73–91
[15] Xu L., Yang Q.: 'Multi-field coupled dynamics for a micro beam', *Mech. Based Des. Struct. Mach.*, 2015, **43**, (1), pp. 57–73
[16] Sabet A., Jabbari A., Sedighi M.: 'Microstructural properties and mechanical behavior of magnesium/hydroxyapatite biocomposite under static and high cycle fatigue loading', *J. Compos. Mater.*, 2018, **52**, (13), pp. 1711–1722
[17] Apuzzo A., Barretta R., Fabbrocino F., *ET AL.* 'Axial and torsional free vibrations of elastic nano-beams by stress-driven two-phase elasticity', *J. Appl. Comput. Mech.*, 2019, **5**, (2), pp. 402–413
[18] Demir Ç., Civalek Ö.: 'A new nonlocal FEM via Hermitian cubic shape functions for thermal vibration of nano beams surrounded by an elastic matrix', *Compos. Struct.*, 2017, **168**, pp. 872–884
[19] Barretta R., Caporale A., Faghidian S.A., *ET AL.*: 'A stress-driven local-nonlocal mixture model for Timoshenko nano-beams', *Compos. B, Eng.*, 2019, **164**, pp. 590–598
[20] Barretta R., de Sciarra F.M., Vaccaro M.S.: 'On nonlocal mechanics of curved elastic beams', *Int. J. Eng. Sci.*, 2019, **144**, p. 103140
[21] Ghorbanfekr-Kalashami H., Neek-Amal M., Peeters F.M.: 'N-doped graphene: polarization effects and structural properties', *Phys. Rev. B*, 2016, **93**, (17), p. 174112
[22] Han T., Luo Y., Wang C.: 'Effects of Si, N and B doping on the mechanical properties of graphene sheets', *Acta Mech. Solida Sin.*, 2015, **28**, (6), pp. 618–625
[23] Mortazavi B., Ahzi S., Toniazzo V., *ET AL.*: 'Nitrogen doping and vacancy effects on the mechanical properties of graphene: a molecular dynamics study', *Phys. Lett. A*, 2012, **376**, (12), pp. 1146–1153
[24] Okamoto S., Ito A.: 'Investigation of mechanical properties of nitrogen-containing graphene using molecular dynamics simulations', Proceedings of the International Multi Conference of Engineers and Computer Scientists Volume I & Volume II, Hong Kong, 2012, pp. 350–355
[25] Chan Y., Hill J.: 'Modelling interaction of atoms and ions with graphene', *Micro Nano Lett.*, 2010, **5**, (5), pp. 247–250
[26] Mortazavi B., Ahzi S.: 'Molecular dynamics study on the thermal conductivity and mechanical properties of boron doped graphene', *Solid State Commun.*, 2012, **152**, (15), pp. 1503–1507
[27] Sedighi H.M., Bozorgmehri A.: 'Dynamic instability analysis of doubly clamped cylindrical nanowires in the presence of Casimir attraction and surface effects using modified couple stress theory', *Acta Mech.*, 2016, **227**, (6), pp. 1575–1591
[28] Barretta R., Faghidian S.A., de Sciarra F.M.: 'Stress-driven nonlocal integral elasticity for axisymmetric nano-plates', *Int. J. Eng. Sci.*, 2019, **136**, pp. 38–52
[29] Numanoglu H.M., Akgoz B., Civalek O.: 'On dynamic analysis of nanorods', *Int. J. Eng. Sci.*, 2018, **130**, pp. 33–50
[30] Akgoz B., Civalek O.: 'A size-dependent beam model for stability of axially loaded carbon nanotubes surrounded by Pasternak elastic foundation', *Compos. Struct.*, 2017, **176**, pp. 1028–1038
[31] de Sciarra F.M., Barretta R.: 'A new nonlocal bending model for Euler–Bernoulli nanobeams', *Mech. Res. Commun.*, 2014, **62**, pp. 25–30
[32] Civalek O., Demir C.: 'A simple mathematical model of microtubules surrounded by an elastic matrix by nonlocal finite element method', *Appl. Math. Comput.*, 2016, **289**, pp. 335–352
[33] Mirakhory M., Khatibi M., Sadeghzadeh S.: 'Vibration analysis of defected and pristine triangular single-layer graphene nanosheets', *Cur. Appl. Phys.*, 2018, **18**, (11), pp. 1327–1337
[34] Kinaci A., Haskins J.B., Sevik C., *ET AL.*: 'Thermal conductivity of BN-C nanostructures', *Phys. Rev. B*, 2012, **86**, (11), p. 115410
[35] Islam M.S., Ushida K., Tanaka S., *ET AL.*: 'Effect of boron and nitrogen doping with native point defects on the vibrational properties of graphene', *Comput. Mater. Sci.*, 2014, **94**, pp. 35–43
[36] Jiang J.W., Wang J.S., Li B.: 'Young's modulus of graphene: a molecular dynamics study', *Phys. Rev. B*, 2009, **80**, (11), p. 113405
[37] Polyanin A.D., Nazaikinskii V.E.: 'Handbook of linear partial differential equations for engineers and scientists' (Chapman and Hall/CRC, Boca Raton, FL, USA, 2015)
[38] Wenzel H.: 'Health monitoring of bridges' (John Wiley and Sons, Hoboken, NJ, USA, 2008)
[39] Zhang L., Brincker R.: 'An overview of operational modal analysis: major development and issues'. 1st Int. Operational Modal Analysis Conf., Copenhagen, Denmark, 2005, pp. 179–190
[40] Brincker R., Zhang L., Andersen P.: 'Modal identification from ambient responses using frequency domain decomposition'. Proc. 18th Int. Modal Analysis Conf. (IMAC), San Antonio, Texas, 2000
[41] Brincker R., Zhang L., Andersen P.: 'Modal identification of output-only systems using frequency domain decomposition', *Smart Mater. Struct.*, 2001, **10**, (3), p. 441
[42] Ewins D.J.: 'Modal testing: theory and practice' (Research Studies Press, Letchworth, 1984)
[43] Available at https://lammps.sandia.gov/
[44] Chen D.: 'Atomic scale details of defect-boundary interactions' (Texas A&M University, USA, 2014)
[45] Sadeghzadeh S.: 'Equivalent mechanical boundary conditions for single layer graphene sheets', *Micro Nano Lett.*, 2016, **11**, (5), pp. 248–252
[46] Sadeghzadeh S., Khatibi M.M.: 'Effects of physical boundary conditions on the transverse vibration of single-layer graphene sheets', *Appl. Phys. A*, 2016, **122**, (9), p. 796
[47] Mortazavi B., Fan Z., Pereira L.F.C., *ET AL.*: 'Amorphized graphene: a stiff material with low thermal conductivity', *Carbon*, 2016, **103**, pp. 318–326
[48] Huheey J., Cottrell T.: 'The strengths of chemical bonds' (Butterworths, London, MA, USA, 1958)
[49] Pradhan S., Phadikar J.: 'Nonlocal elasticity theory for vibration of nanoplates', *J. Sound Vib.*, 2009, **325**, (1-2), pp. 206–223
[50] Rao S.S.: 'Vibration of continuous systems' (Wiley Online Library, Hoboken, NJ, USA, 2007)
[51] Timoshenko S.P., Gere J.M.: 'Theory of elastic stability' (Courier Corporation, North Chelmsford, MA, USA, 2009)